Benomyl and Colchicine Synergistically Inhibit Cell Proliferation and Mitosis: Evidence of Distinct Binding Sites for These Agents in Tubulin[†]

Marie-Jeanne Clément,[‡,§] Krishnan Rathinasamy,[§,||] Elisabeth Adjadj,[‡] Flavio Toma,[‡] Patrick A. Curmi,*[,‡] and Dulal Panda*[,||]

Laboratoire Structure et Activité des Biomolécules Normales et Pathologiques, INSERM U829, Université Evry-Val d'Essonne, EA3637, Evry, F-91025 France, and School of Biosciences and Bioengineering, Indian Institute of Technology Bombay, Mumbai, India 400076

Received June 17, 2008; Revised Manuscript Received October 28, 2008

ABSTRACT: Benomyl, a tubulin-targeted antimitotic antifungal agent, belongs to the benzimidazole group of compounds, which are known to inhibit the binding of colchicine to tubulin. Therefore, benomyl was thought to bind at or near the colchicine-binding site on tubulin. However, recent mutational studies in yeast and fluorescence studies involving competitive binding of benomyl and colchicine on goat brain tubulin suggested that benomyl may bind to tubulin at a site distinct from the colchicine-binding site. We set out to examine whether colchicine and benomyl bind to tubulin at distinct sites using a human cervical cancer (HeLa) cell line with the thinking that these agents should exert either additive or synergistic activity on cell proliferation if their binding sites on tubulin are different. We found that benomyl and colchicine synergistically inhibited the proliferation of HeLa cells and blocked their cell cycle progression at mitosis. The synergistic activity of benomyl and colchicine was also apparent from their strong depolymerizing effects on both the spindle and interphase microtubules when used in combinations, providing further evidence that these agents bind to tubulin at different sites. Using NMR spectroscopy, we finally demonstrated that benomyl and colchicine bind to tubulin at different sites and that the binding of colchicine seems to positively influence the binding of benomyl to tubulin and vice versa. Further, an analysis of the saturation transfer difference NMR data yielded an interesting insight into the colchicine−tubulin interaction. The data presented in this study provided a mechanistic understanding of the synergistic effects of benomyl and colchicine on HeLa cell proliferation.

Benomyl [methyl 1-(butylcarbamoyl)benzimidazol-2-yl-carbamate], a microtubule-targeted fungicide, belongs to a group of compounds called benzimidazoles. It was extensively used as an agricultural fungicide on a variety of food crops like fruits and vegetables and on ornamental plants (*1*). Benomyl is unstable in aqueous solutions and decomposes into its metabolite carbendazim, which is also functionally active (*2, 3*). Moreover, benomyl is known to inhibit mitosis in fungal (*1, 4*) and mammalian cells (*5, 6*) by targeting microtubules and inhibiting their proliferation. Benomyl is considered to be relatively less toxic to mammalian cells because of its moderate affinity for mammalian tubulin rather than fungal tubulin (*7*). Microtubules, the dynamic cytoskeletal polymers of eukaryotic cells, are composed of α- and β-tubulin heterodimers, and they play vital roles in various cellular functions. Hence, microtubules remain an attractive target for various diseases, including cancer and fungal diseases (*8, 9*).

Benomyl is shown to suppress the assembly of spindle microtubules in HeLa cells (*6*). At its half-maximal proliferation inhibitory concentration (IC_{50}),[1] benomyl did not significantly depolymerize the interphase microtubules in HeLa cells (*5, 6*); however, it perturbed the chromosomal alignment at the metaphase plate and microtubule−kinetochore interactions and caused loss of tension across the sister kinetochores (*6*). It was also shown to suppress the dynamic instability of microtubules in MCF-7 cells and to increase the level of nuclear accumulation of p53 (*10*). In vitro, benomyl is reported to inhibit the polymerization of tubulin into microtubules and to suppress the dynamic instability of bovine brain microtubules (*5*). Benomyl binds to mammalian tubulin with a modest affinity, and the binding is shown to cause a conformational change in tubulin as judged by the alteration of the secondary structure of tubulin (*5*).

The exact binding site of benomyl on tubulin is not yet known. Benomyl was suggested to bind at or near the colchicine-binding site since it belongs to the benzimidazole group of compounds which are known to inhibit the binding

[†] This work is partly supported by the Association pour la Recherche sur le Cancer (ARC) and partly supported by a grant from the Department of Biotechnology, Government of India. M.-J.C. is the recipient of a postdoctoral fellowship from Région Ile-de-France.

* To whom correspondence should be addressed. P.A.C.: phone, 33 (0)1 69 47 01 87; fax, 33 (0)1 69470219; e-mail, pcurmi@univ-evry.fr. D.P.: phone, 91-222576-7838/7770; fax, 91-222572-3480; e-mail, panda@iitb.ac.in.

[‡] INSERM/UEVE U829.

[§] These authors contributed equally to this work.

[||] Indian Institute of Technology Bombay.

[1] Abbreviations: IC_{50}, half-maximal inhibitory concentration; STD, saturation transfer difference; BSA, bovine serum albumin; PBS, phosphate-buffered saline; DMSO, dimethyl sulfoxide; CI, combination index; CBZ, carbendazim; DBU, dibutylurea; SD, standard deviation.

10.1021/bi801136q CCC: $40.75
Published on Web 11/20/2008

of colchicine on tubulin both competitively and noncompetitively (*11, 12*). It was hypothesized that the benomyl-binding site is located in the core of β-tubulin at a site distinct from the colchicine site based on site-directed mutation studies of the β-tubulin gene in *Saccharomyces cerevisiae* (*13*). Using fluorescence spectroscopy, it was reported that benomyl did not perturb the kinetics of colchicine binding to tubulin and that the preincubation of tubulin with benomyl did not affect the binding of colchicine to tubulin (*5*). Furthermore, this study provided evidence indicating that benomyl could bind to the preformed tubulin−colchicine complex. The results together suggested that benomyl binds to tubulin at a site distinct than the colchicine-binding site (*5*). However, these are indirect studies involving colchicine fluorescence and 1-anilinonaphthalene-8-sulfonic acid fluorescence.

If benomyl and colchicine could bind to tubulin simultaneously, it is reasonable to hypothesize that they will exert either a synergistic effect or an additive effect on cell proliferation. We found here that benomyl and colchicine indeed synergistically inhibited the proliferation of HeLa cells and blocked the cell cycle progression at mitosis. The synergistic activity of benomyl and colchicine was also clear from their strong disruptive effects on both the spindle and interphase microtubules, while the individual agents had minimal effects under similar conditions. This is supported by saturation transfer difference (STD) NMR (*14*) data that show benomyl and colchicine bind to tubulin at different sites and that the binding of one ligand seems to positively affect the binding of the other ligand. Taken together, the synergistic effects observed with benomyl and colchicine in cells may be explained by the cooperative interaction of both drugs on tubulin. The data presented in this study lead to the conclusion that the combination of benomyl with a tubulin-targeted agent such as colchicine may have beneficial therapeutic effects.

MATERIALS AND METHODS

Materials. Benomyl was purchased from Sigma-Aldrich (Milwaukee, WI) and colchicine from Acros Organics (Ceel, Belgium). Mouse monoclonal anti-α-tubulin IgG, Hoechst 33258, and bovine serum albumin (BSA) were purchased from Sigma (St. Louis, MO). Anti-mouse IgG−Alexa 568 conjugate was purchased from Molecular Probes (Eugene, OR). Minimal essential medium (MEM), phosphate-buffered saline (PBS), and an endotoxin free antibiotic solution were purchased from Hi Media (Mumbai, India). All other reagents used were of analytical grade.

Cell Culture and Cell Proliferation Assay. HeLa cells were grown in minimal essential medium (Hi Media) supplemented with 10% (v/v) fetal bovine serum and sodium bicarbonate (2.0 mg/mL) in the presence of antibiotics (100 units of penicillin, 0.1 mg of streptomycin, and 0.25 μg of amphotericin B per milliliter of medium) at 37 °C in a humidified atmosphere of 5% CO_2 and 95% air (*6*). Benomyl and colchicine were freshly prepared by being dissolved in 100% dimethyl sulfoxide (DMSO); the final DMSO concentration in all experiments was 0.1%. The effects of benomyl and colchicine and their combination on cell proliferation were determined in 24-well tissue culture plates by counting the cells using a hemocytometer (*15*). Briefly, cells were seeded at a density of 1×10^5 cells/mL, and after 24 h, the medium was replaced with fresh medium containing 0.1% DMSO vehicle (control) or benomyl or colchicine or benomyl and colchicine in combination and incubated for an additional 24 h. Both attached and unattached cells were harvested and combined after trypsinization (0.025% trypsin and 0.037% EDTA for 10 min) and counted in the presence of trypan blue in a hemocytometer to determine the percent inhibition of proliferation (*15*).

Immunofluorescence Microscopy. Immunofluorescence microscopy was performed as described previously (*6*). Cells were seeded on glass coverslips at a density of 6×10^4 cells/mL in 24-well tissue culture plates. After 24 h of drug treatment, cells were fixed in 3.7% formaldehyde for 30 min at 37 °C and then treated with cold 100% methanol (−20 °C) for 10 min. After the nonspecific binding sites had been blocked with a 2% BSA/PBS mixture, cells were incubated with mouse monoclonal anti-α-tubulin IgG (Sigma) at a 1:300 dilution for 2 h at room temperature (RT). Coverslips were then rinsed with the BSA/PBS mixture and incubated with anti-mouse IgG−Alexa 568 conjugate (Molecular Probes) at a 1:300 dilution for 1 h at RT. Coverslips were then rinsed with PBS and incubated with Hoechst 33258 (1 μg/mL) for 8 min at 25 °C. The microtubules and DNA were observed with a Nikon Eclipse TE-2000 U microscope (Nikon, Kanagawa, Japan). The images were analyzed using Image Pro-Plus (Media Cybernetics, Silver Spring, MD).

Mitotic Index. Cells were grown on coverslips as described, treated with the drugs for 24 or 48 h, and then centrifuged in a Labofuge 400R cytospin (Heraeus, Hanau, Germany) for 10 min to sediment any floating or loosely attached cells, fixed with 3.7% formaldehyde for 20 min at RT, and washed with PBS. Cells were then permeabilized with ice-cold methanol and stained with Hoechst 33258. The number of cells in the mitotic phase, cells containing multiple nuclei, cells containing micronuclei, and normal interphase cells were counted under the Eclipse TE-2000 U microscope (Nikon) using the fluorescence of Hoechst 33258. At least 500 cells were scored for each concentration of the drugs.

Determination of the Combination Index (CI). HeLa cells were treated with different concentrations of benomyl, colchicine, or colchicine with benomyl, for 24 h. The CI was determined in an effort to examine whether the combination of the two drugs inhibited HeLa cell proliferation synergistically, additively, or antagonistically. The CI was calculated by the Chou and Talalay method (*16, 17*), using the equation

$$\mathrm{CI} = \frac{(D)1}{(\mathrm{Dx})1} + \frac{(D)2}{(\mathrm{Dx})2}$$

where $(D)1$ and $(D)2$ are the concentrations of drug 1 (colchicine) and drug 2 (benomyl), respectively, in combination that produce a given effect, and $(\mathrm{Dx})1$ and $(\mathrm{Dx})2$ are the concentrations of drugs 1 and 2, respectively, that also produce the same effect when used alone.

(Dx), the concentration of the drug which produces any particular effect, was calculated from the median effect equation of Chou et al. (*18*)

$$(\mathrm{Dx}) = D_m[f_a/f_u]^{1/m}$$

where D_m is the median dose, f_a is the fraction affected, and f_u is the fraction unaffected ($f_u = 1 - f_a$).

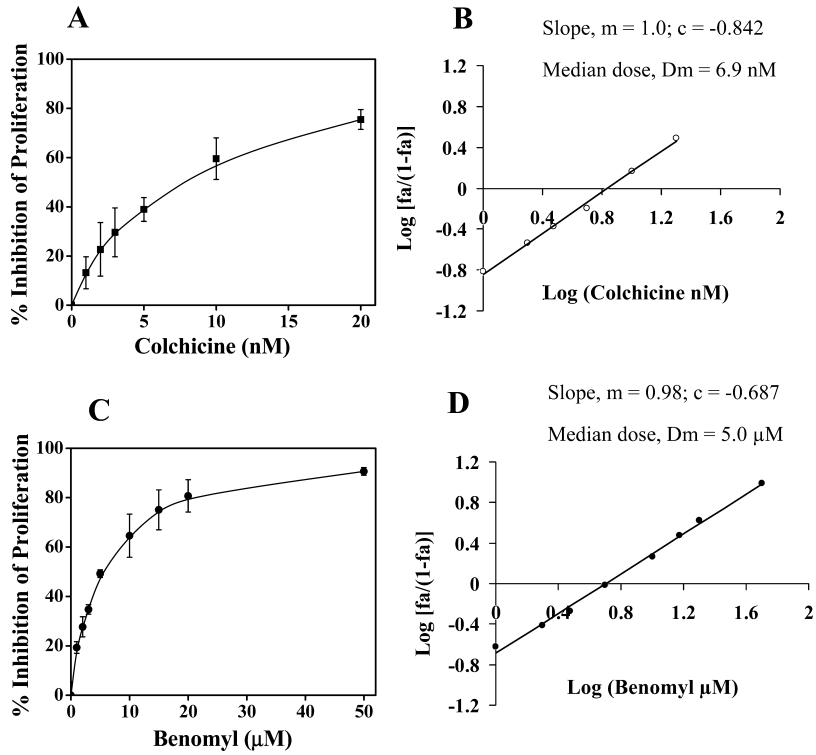

FIGURE 1: Benomyl and colchicine inhibited HeLa cell proliferation. HeLa cells were incubated with the indicated concentration of the drugs for 24 h. The percent inhibition of cell proliferation was calculated after the cells had been counted under a microscope in the presence of trypan blue dye. Inhibition of cell proliferation (A) and median effect plot for the inhibition of cell proliferation (B) in the presence of colchicine. Inhibition of cell proliferation (C) and median effect plot for the inhibition of cell proliferation (D) in the presence of benomyl. Data are averages of four independent experiments, and error bars represent the SD.

Median dose D_m was obtained from the antilog of the X-intercept of the median effect plot, where $X = \log(D)$ versus $Y = \log(f_a/f_u)$; i.e., $D_m = 10^{-(Y\text{-intercept})/m}$, where m is the slope of the median effect plot.

A CI of <1 indicates synergism, a CI of 1 additivity, and a CI of >1 antagonism.

Purification of Tubulin. Tubulin was purified from sheep brain using the method of Castoldi and Popov (*19*) and stored at −80 °C. Before use, the tubulin stock was thawed, and an additional cycle of polymerization was performed. The tubulin concentration was determined by spectrophotometry using an extinction coefficient of 1.2 L g^{-1} cm^{-1} at 278 nm (*20*).

NMR Spectroscopy. All ^{1}H NMR experiments were performed at 293 K on a Bruker Avance 600 MHz NMR spectrometer equipped with a cryoprobe, and data were processed using XWINNMR (Bruker). Benomyl and colchicine stock solutions (20 mM) were prepared in DMSO. To acquire the spectra of free benomyl and colchicine, we dissolved the stock solution to either 500 μM or 1.4 mM in 50 mM sodium phosphate buffer (pH 6.8) in 10% D_2O. To study the interaction of benomyl and/or colchicine with tubulin, we prepared a 46:1 benomyl/tubulin or colchicine/tubulin solution (1.4 mM benomyl and/or colchicine and 30 μM tubulin), in 50 mM sodium phosphate buffer (pH 6.8) in 10% D_2O. For the competition experiments, 30 μM tubulin was preincubated with 200 μM benomyl or colchicine for 1 h at room temperature before the addition of the other drug. To detect nonspecific benomyl−protein interactions, we analyzed a control sample prepared in the same way using BSA. One-dimensional proton spectra were acquired with 32 scans and 16K data points. One-dimensional (1D) STD−NMR experiments (*14*) with benomyl or colchicine in interaction with tubulin were conducted with 4096 scans. The protein resonances were saturated at 10 ppm (40 ppm for reference spectra) with a cascade of 40 selective Gaussian-shaped pulses with a duration of 50 ms with a 1 ms delay between each pulse, resulting in a total saturation time of 2.04 s. A STD control experiment was performed with colchicine alone to ensure that tubulin saturation at 10 ppm was selective enough not to induce an artifact saturation of the colchicine proton at 8.9 ppm (data not shown). Subtraction of the saturated spectra from the reference spectra was performed by phase cycling. STD enhancement values were calculated by dividing the STD signal intensities by the intensities of the corresponding signals in the one-dimensional spectra and then normalized in relation to the largest value. In all experiments, suppression of the water signal was achieved with the WATERGATE sequence before acquisition (*21*).

RESULTS

Benomyl Synergistically Inhibits the Proliferation of HeLa Cells in Combination with Colchicine. Colchicine inhibited the proliferation of HeLa cells in a concentration-dependent manner with a half-maximal inhibitory concentration (IC_{50}) of ~7 nM (Figure 1A) and a median inhibitory dose of 6.9 nM (Figure 1B). For example, 3 and 10 nM colchicine inhibited cell proliferation by 30 and 60%, respectively. As previously documented (*5, 6*), benomyl inhibited HeLa cell proliferation in a concentration-dependent fashion with an IC_{50} of ~5 μM and a median inhibitory dose of 5 μM (Figure 1C,D). In the presence of 3 and 10 μM benomyl, the

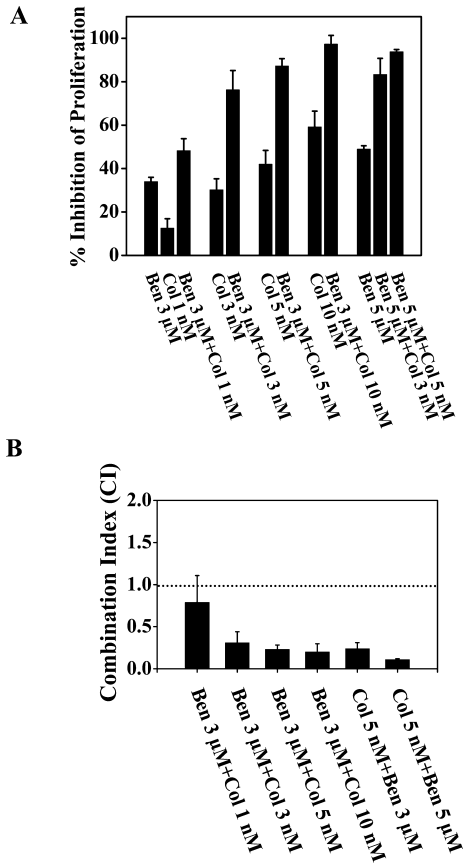

FIGURE 2: Combination of benomyl and colchicine that exerted synergistic effects on HeLa cell proliferation. The effects of the combination of benomyl (Ben) and colchicine (Col) on HeLa cell proliferation after a 24 h treatment are shown in panel A. The combined effects of colchicine and benomyl on HeLa cell proliferation were analyzed using the Chou and Talalay equation as described in Materials and Methods. The combination indices at different drug concentrations are shown in panel B. Data are averages of four experiments, and error bars represent the SD.

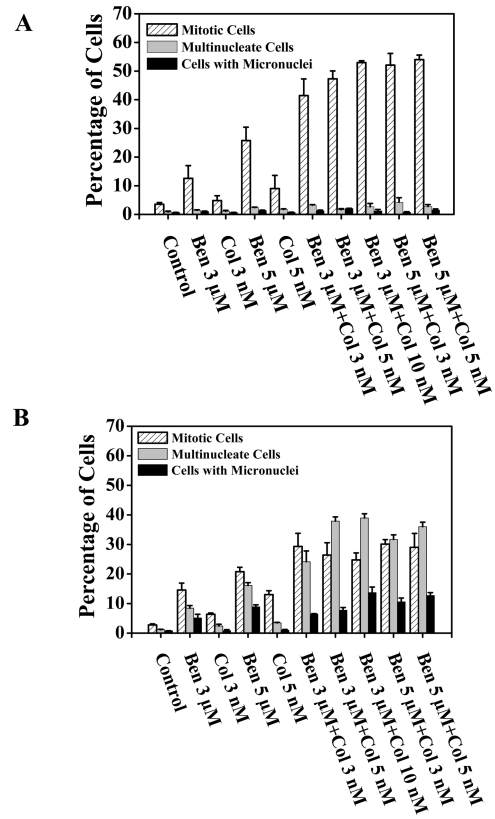

FIGURE 3: Combination of benomyl and colchicine that strongly induce mitotic block. HeLa cells were incubated with the vehicle or indicated concentration of benomyl (Ben), colchicine (Col), or benomyl and colchicine for 24 (A) or 48 h (B). The percentage of cells blocked at mitosis (average of five different experiments) and the percentage of cells containing multiple nuclei and micronulei (average of three different experiments) were calculated as mentioned in Materials and Methods. Error bars represent the SD.

proliferation of HeLa cells was inhibited by 34 and 65%, respectively. To establish a quantitative relationship between the combination of benomyl and colchicine, the combination index (CI) was calculated on the basis of the Chou and Talalay equation (*18*) as described in Materials and Methods. The CI for the combination of 3 μM benomyl and 1 nM colchicine was found to be $\sim 0.8 \pm 0.3$. When colchicine and benomyl were combined as 3 μM benomyl and 3 nM colchicine, the level of inhibition of cell proliferation was found to be 76% (Figure 2A) and the CI with this combination was calculated to be 0.31 ± 0.13 (Figure 2B). The combination of 3 μM benomyl and 5 nM colchicine or 3 μM benomyl and 10 nM colchicine was also found to be strongly synergistic with CI values of 0.23 ± 0.05 and 0.2 ± 0.1, respectively (Figure 2B). The combination of 5 μM benomyl with 3 or 5 nM colchicine was also found to be strongly synergistic with a CI value of 0.29 or 0.11, respectively (Figure 2B).

The Combination of Benomyl and Colchicine Potently Induces Mitotic Arrest in HeLa Cells. After a 24 h treatment, control cells had 3.5% of their population in mitosis. Under similar conditions, benomyl (3 μM) and colchicine (3 nM) when used alone produced 12.5 and 5% mitotic block, respectively (Figure 3A). The mitotic index was found to be 41% when 3 μM benomyl was combined with 3 nM colchicine. Further, 5 μM benomyl and 5 nM colchicine induced a mitotic block of $\sim$25 and $\sim$9%, respectively, when used alone, while the combination of benomyl and colchicine at these concentrations induced a mitotic block of $\sim$54% (Figure 3A). The cells were also analyzed for other abnormalities like multinucleated cells and apoptotic cells containing micronuclei. After a 24 h treatment with the drug combinations, the number of cells with multiple nuclei and micronuclei did not differ significantly from the control treatment (Figure 3A).

To further analyze whether the cells were failing in cytokinesis, we scored the number of multinucleated cells after exposing the HeLa cells to benomyl, colchicine, or a drug combination for 48 h (approximately two cell cycles). The percentages of multinucleated cells and cells containing micronuclei were found to increase significantly (Figure 3B). For example, in the presence of 3 μM benomyl and 5 nM colchicine, 26% of the cells were found to be at mitosis, 38% of the cells had multiple nuclei, and 8% of the cells had micronuclei (Figure 3B). Nearly all mitotic cells were found to be irregular, indicating that 72% of the total cells were abnormal. The results suggested that the combinations of benomyl and colchicine strongly induced mitotic block after a 24 h drug treatment, and the prolonged treatment for 48 h increased the number of multinucleated cells as a consequence of an aberrant mitotic exit without them undergoing cytokinesis.

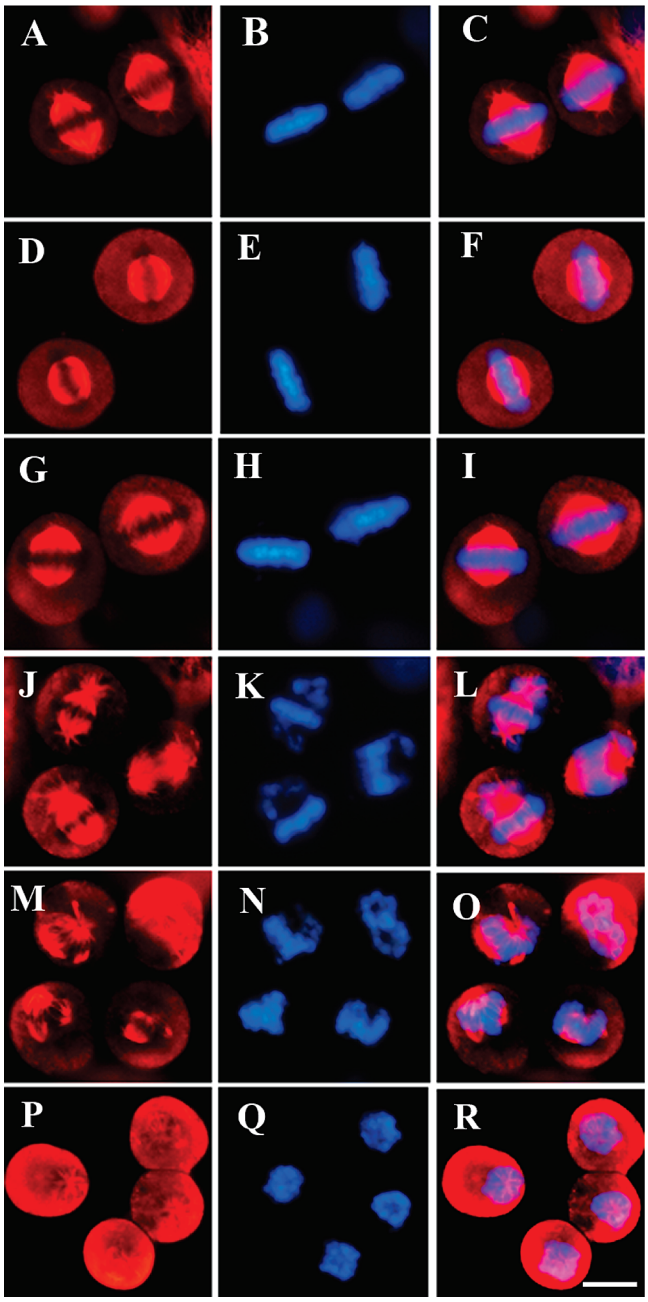

FIGURE 4: Effects of benomyl and colchicine on the spindle organization when used alone and in combination. HeLa cells were treated with the vehicle, benomyl, colchicine, or benomyl and colchicine together and incubated for 24 h and then fixed and processed to visualize tubulin (red) and DNA (blue). The organization of spindles in control cells (0.1% DMSO) (A) and in cells treated with 3 μM benomyl (D), 3 nM colchicine (G), 3 μM benomyl and 3 nM colchicine (J), 3 μM benomyl and 5 nM colchicine (M), and 3 μM benomyl and 10 nM colchicine (P) is shown. Panels B, E, H, K, N, and Q show the chromosomal organization of the cells corresponding to panels A, D, G, J, M, and P, respectively. Panels C, F, I, L, O, and R show the merged images of spindles and chromosomes. The bar is 10 μm.

A Combination of Benomyl and Colchicine Exhibits a Stronger Depolymerizing Effect on the Spindles Than Either of the Drugs When Used Alone. Control mitotic HeLa cells exhibited normal spindles with the chromosomes aligned compactly at the metaphase plate (Figure 4A−C). When used alone, 3 μM benomyl (Figure 4D−F) or 3 nM colchicine (Figure 4G−I) did not disrupt the organization of microtubules and DNA. Most of the mitotic cells treated with 3 μM benomyl or 3 nM colchicine exhibited normal bipolar spindles with the chromosomes organized at the metaphase plates except in a few cells where one or two chromosomes were not aligned at the metaphase plate. Most of the cells treated with 5 nM colchicine also exhibited normal bipolar spindles (data not shown). The combined use of benomyl and colchicine disrupted the organization of the microtubules and chromosomes. In cells treated with 3 μM benomyl and 3 nM colchicine together, almost all the cells had misaligned chromosomes and abnormal spindles (Figure 4J−L). In the cells treated with 3 μM benomyl and 5 nM colchicine, the spindle microtubules were significantly depolymerized (Figure 4M−O). The combination 3 μM benomyl and 10 nM colchicine completely depolymerized the spindles, giving the appearance of c-type mitosis having no spindles and a rounded mass of chromosomes (Figure 4P−R).

Cells treated with 3 μM benomyl (Figure 5B), 3 nM colchicine (Figure 5C), or 5 nM colchicine (Figure 5D) exhibited a nearly normal interphase microtubular network as observed in the control cells (Figure 5A). However, the interphase microtubules of the cells treated with 10 nM colchicine (Figure 5E) were moderately depolymerized. The combinations of 3 μM benomyl and 3 nM colchicine (Figure 5F) and 3 μM benomyl and 5 nM colchicine (Figure 5G) induced a moderate depolymerization of the interphase microtubules, while the combination of 3 μM benomyl and 10 nM colchicine induced significant depolymerization of the interphase microtubules (Figure 5H).

Investigation of the Interaction of Benomyl and Tubulin by NMR Spectroscopy. We previously showed that benomyl binds to tubulin with a modest affinity (K_d, 12 μM) and does not compete with the colchicine site (*5*). In addition to these data, we designed here STD−NMR experiments (*14*) to check directly the interaction of benomyl with tubulin and the possibility that benomyl and colchicine compete for the same binding site. As a preliminary step to the benomyl−tubulin interaction study by NMR, we projected to attribute the resonances of free benomyl in tubulin compliant buffer. However, we observed on the 1D spectrum that resonances did not correspond fully to the molecular structure of benomyl (Figure 6A). Indeed, we expected four signals between 7 and 9 ppm corresponding to the four protons of the benzimidazole ring of benomyl, which would resonate differently due to the presence of the butylaminocarbonyl group, but we observed only two resonance peaks. Moreover, the protons of the butyl chain (between 0 and 4 ppm) were weaker than expected. It is well-known that benomyl can be degradated into lower-molecular weight products (Figure 6B) (*22, 23*). We used this information to fully attribute the 1D spectra. We observed that under the conditions used during the preparation of the NMR sample and experiments (~20 min), benomyl is very unstable and is degradated to carbendazim (CBZ) and butyl isocyanate (volatile product) (Figure 6A). We also noticed that the stock solution in DMSO is completely degraded in CBZ and dibutylurea (DBU) after 1 week (Figures 1S and 2S of the Supporting Information) and that these compounds were stable in the tubulin compliant buffer (Figure 6C). The benomyl−tubulin interaction was thus investigated using this stock solution.

STD−NMR experiments were performed to identify the protons of benomyl in rapid interaction with tubulin. When benomyl was added to tubulin, we found that protons of CBZ

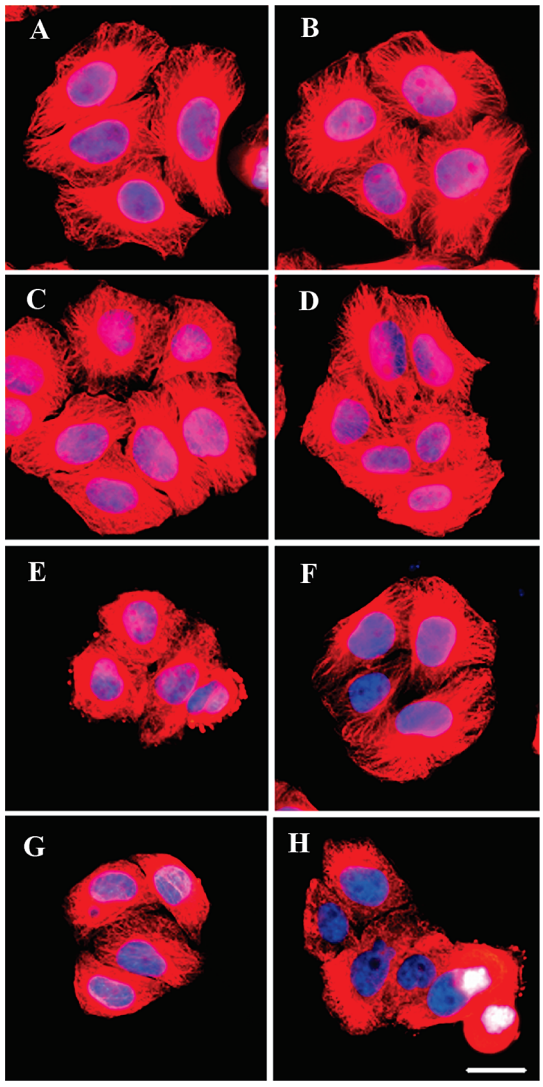

FIGURE 5: Effects of benomyl and colchicine on the interphase microtubule organization when used alone and in combination. HeLa cells were treated with the vehicle or benomyl or colchicine or benomyl and colchicine together and incubated for 24 h and then fixed and processed to visualize tubulin (red) and DNA (blue). The merged images of microtubules and chromosomal organization of control cells (0.1% DMSO) (A) and cells treated with 3 μM benomyl (B), 3 nM colchicine (C), 5 nM colchicine (D), 10 nM colchicine (E), 3 μM benomyl and 3 nM colchicine (F), 3 μM benomyl and 5 nM colchicine (G), and 3 μM benomyl and 10 nM colchicine (H) is shown. The bar is 20 μm.

and DBU interacted with tubulin (Figure 7A,B) and the most strongly enhanced signals correspond to the protons of the benzimidazole ring of CBZ (Table 1). The specificity of these interactions was probed using BSA as a control instead of the tubulin target. In this case, while DBU still interacts through similar contacts with BSA, we found that CBZ does not interact with BSA (Figure 7C). Together, these data are in agreement with a specific CBZ−tubulin interaction and suggest that the functional activity of benomyl is due to the CBZ compound.

It has been hypothesized that benomyl and colchicine compete for the same site on tubulin. To test this hypothesis, we repeated the STD−NMR experiments using benomyl and tubulin that was preincubated with an excess of colchicine to saturate the colchicine-binding site. If benomyl actually competes with colchicine, preincubation of tubulin with colchicine should impede its binding to tubulin. The results clearly show that this is not the case. Indeed, the 1D STD−NMR spectrum (Figure 7D) shows that all nonexchangeable protons of CBZ remain in interaction with tubulin in the tubulin−colchicine complex, and interestingly, we observed that the STD signals of protons A−C were enhanced by factors of 1.4, 1.5, and 1.1, respectively (Table 1). With regard to DBU, though the magnitudes of its STD signals were decreased in the presence of the tubulin−colchicine complex (Table 1), we demonstrated, using BSA, that its interaction with tubulin is not specific. Thus, benomyl/CBZ seems not to compete with colchicine, and its binding to tubulin seems even to be improved with the presence of colchicine.

To fully document the mutual influence of each of these drugs on the interaction with tubulin, we then explored the possibility that benomyl/CBZ may influence the binding of colchicine on tubulin. We thus first recorded the 1D spectrum of colchicine via 1D STD−NMR experiments with colchicine in the presence of tubulin. The assignment of colchicine protons was straightforward (Figure 8A). The 1D STD−NMR spectrum revealed that methoxy protons 2 and 3 of ring A and proton 12 of ring C are the most enhanced, suggesting a proximity of these protons with tubulin (Figure 8A,B and Table 2). 1D and 1D STD−NMR experiments were then conducted to study the interaction of colchicine with tubulin that was preincubated with an excess of benomyl. The 1D STD−NMR spectrum (Figure 8C) showed that colchicine still interacted with tubulin in the presence of benomyl. The most enhanced signals of colchicine correspond to the same protons as those enhanced in the STD−NMR spectrum recorded without benomyl (Table 2). Surprisingly, we observed that the STD−NMR signals were on average 2.6 more intense than those without preincubation with benomyl (Table 2). Thus, the presence of benomyl seems to enhance colchicine−tubulin interaction, in agreement with the slight broadening of proton resonances observed in the 1D spectrum (Figure 3S of the Supporting Information). These data confirm that benomyl does not compete with colchicine for its binding to tubulin and suggest that its presence positively influences the binding of colchicine to tubulin.

Together, the NMR data indicate that the benomyl/CBZ binding site on tubulin is different from that of colchicine, and they also show that the presence of one of these drugs likely improves the binding of the other drug.

DISCUSSION

In this study, we found that benomyl and colchicine in combination inhibited HeLa cell proliferation synergistically. The combined use of these two agents also produced depolymerizing effects on the microtubules of HeLa cells stronger than that of the isolated agents when used alone. The inhibitory effect of these drugs on cell proliferation was observed in association with the induction of a metaphase block. Our previous report using fluorescence spectroscopy indicated that benomyl did not inhibit the binding of colchicine to tubulin and that it could bind to the preformed tubulin−colchicine complex (*5*). NMR experiments presented in this work strongly suggested that the benomyl-binding site on tubulin is distinct from the colchicine-binding site and that these agents positively affected the binding of each other to tubulin.

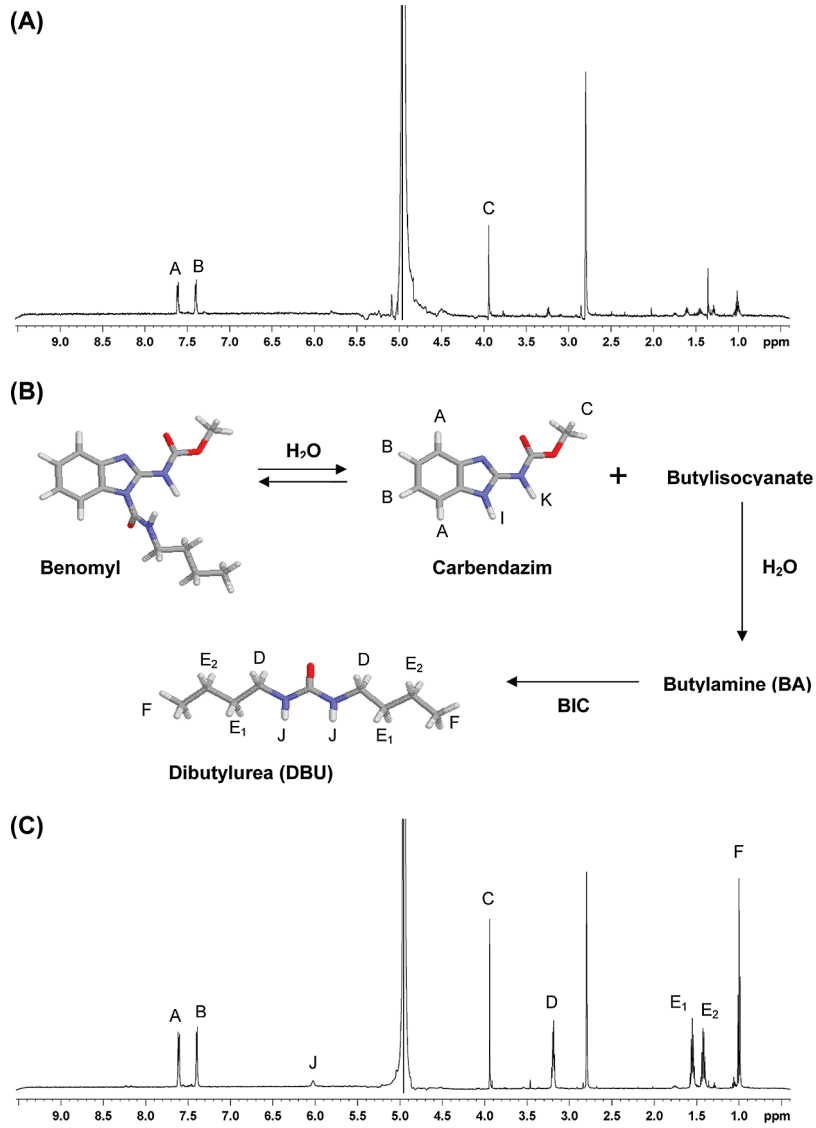

FIGURE 6: Benomyl is degraded in aqueous solution. (A) 1D spectrum recorded after dilution of a benomyl fresh stock solution to 500 μM in 50 mM sodium phosphate buffer (pH 6.8) (10% D_2O). (B) Pathway of benomyl degradation. In aqueous solution, benomyl is converted to carbendazim, butyl isocyanate (BIC), butylamaine (BA), and the combination of BIC and BA form dibutylurea (DBU). (C) 1D spectrum recorded after dilution of a 1-week-old benomyl stock solution to 1.4 mM in 50 mM sodium phosphate buffer (pH 6.8) (10% D_2O). Only resonances of benomyl degradation products are labeled A−J. Protons K and I of CBZ exchange with the solvent and consequently are not visible in the spectrum.

CBZ, the Major Degradation Product of Benomyl, Seems To Be the Active Agent of Benomyl. We wanted to study the interaction between benomyl and tubulin by NMR. Benomyl is known to degrade in aqueous solution (*2, 3*). We also found that benomyl is unstable in aqueous solution and degrades into several degradation products, among which CBZ is the major metabolite. STD−NMR data from this study indicate that this metabolite interacts specifically with tubulin. Several studies suggested that CBZ is probably responsible for in vivo and in vitro effects attributed to benomyl in fungi, plants, or mammalian cells, because it acts by the same mechanism as benomyl (*4, 24, 25*). The NMR results obtained here clearly support this idea.

Interaction of Colchicine with Tubulin Examined by NMR. Interaction of colchicine with tubulin was investigated with STD−NMR experiments. In the spectra, protons of rings A and C gave the most enhanced signals, supporting the fact the interaction is mainly driven by these rings (*26*−*28*). We also contrasted STD data for the crystal structure of the ternary tubulin−colchicine−stathmin-like domain complex (*29*) by comparing the number of intermolecular contacts (<5 Å) of colchicine protons in the crystal with their STD−NMR enhancement value (Table 3). With regard to the methoxy protons of ring A, NMR data and the crystal structure are in agreement; i.e., the most enhanced proton resonances in STD experiments correspond to protons that present the greater number of intermolecular contacts in the crystal structure. However, for protons of ring C, there is some divergence. For example, proton 12, which is significantly enhanced in STD−NMR experiments, makes few contacts in the crystal structure. That could be explained by the conformational flexibility of ring C (*30*−*32*) that may exist in solution. Furthermore, STD data of colchicine obtained with and without benomyl show that the contacts of colchicine with tubulin change in the presence of benomyl (Tables 2 and 3). This finding could be related to the conformational changes of tubulin upon benomyl binding that we previously demonstrated (*5*).

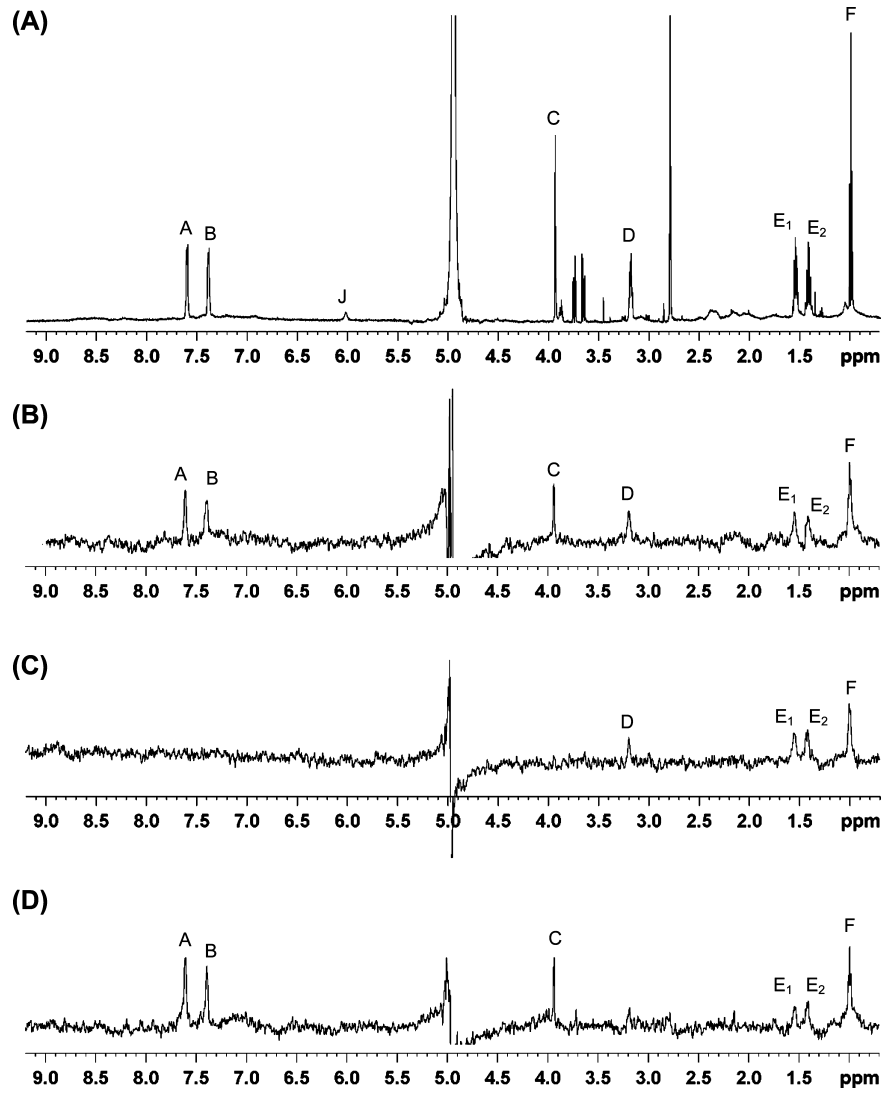

FIGURE 7: CBZ specifically interacts with tubulin, and its binding is improved in the presence of colchicine. (A) 1D ^{1}H NMR spectrum of benomyl degradation products in the presence of tubulin. (B−D) 1D STD−NMR spectra of benomyl degradation products in the presence of tubulin, BSA, and tubulin preincubated with colchicine, respectively. The selective saturation of protein protons has been applied at 10 ppm. Protons affected by the selective saturation of protein are labeled (see Figure 6B for proton assignments).

Table 1: Comparison of STD Enhancements of Benomyl Protons in the Presence of Tubulin Preincubated with Colchicine or Not

			STD enhancement (%)[a]		
compound	proton resonance	δ (ppm)	benomyl with tubulin	benomyl with tubulin−colchicine	colchicine/ non-colchicine ratio
CBZ	A	7.61	73	100	1.4
	B	7.39	59	90	1.5
	C	3.94	40	45	1.1
	I	no[b]	−	−	−
	K	no[b]	−	−	−
DBU	D	3.19	61	25	0.4
	E1	1.55	55	36	0.7
	E2	1.43	54	47	0.9
	F	1.00	45	40	0.9
	J	6.02	0	0	0

[a] Normalized to the strongest enhancement, i.e., resonance A in the presence of tubulin preincubated with colchicine. [b] Not observed.

A Cooperative Interaction between Both Drugs May Explain Their Synergistical Effects Observed in Cells. Low concentrations of benomyl and colchicine when used alone had minimal effects on the mitotic progression; however, these agents when used in combination strongly inhibited cell cycle progression at mitosis, and such low concentrations in combination exerted strong depolymerizing effects on both the mitotic and interphase microtubule networks of the HeLa cells. Since the agents were used at low concentrations, such strong effects can only be possible if one agent potentiates the effects of the other agent on tubulin. Interestingly, NMR competition experiments showed an increase in the magnitudes of the STD−NMR signals when either benomyl or colchicine was mixed with tubulin previously preincubated with the other compound. This observation suggests a positive mutual influence for tubulin binding, consistent with the fact that these compounds act synergistically on HeLa cell proliferation and destabilize the microtubule network in the cell.

It is well-known that colchicine binds to tubulin at the intradimer interface and induces conformational changes in tubulin upon its binding (*13*). The crystal structure of a ternary tubulin−colchicine−stathmin-like domain complex shows that the colchicine-binding site is mostly buried in the β-subunit (*28, 29*). We have previously shown by spectrophotometry and circular dichroïsm that benomyl also induces conformational modifications upon binding to tubulin (*5*), and it is assumed that the benomyl/CBZ-binding site is

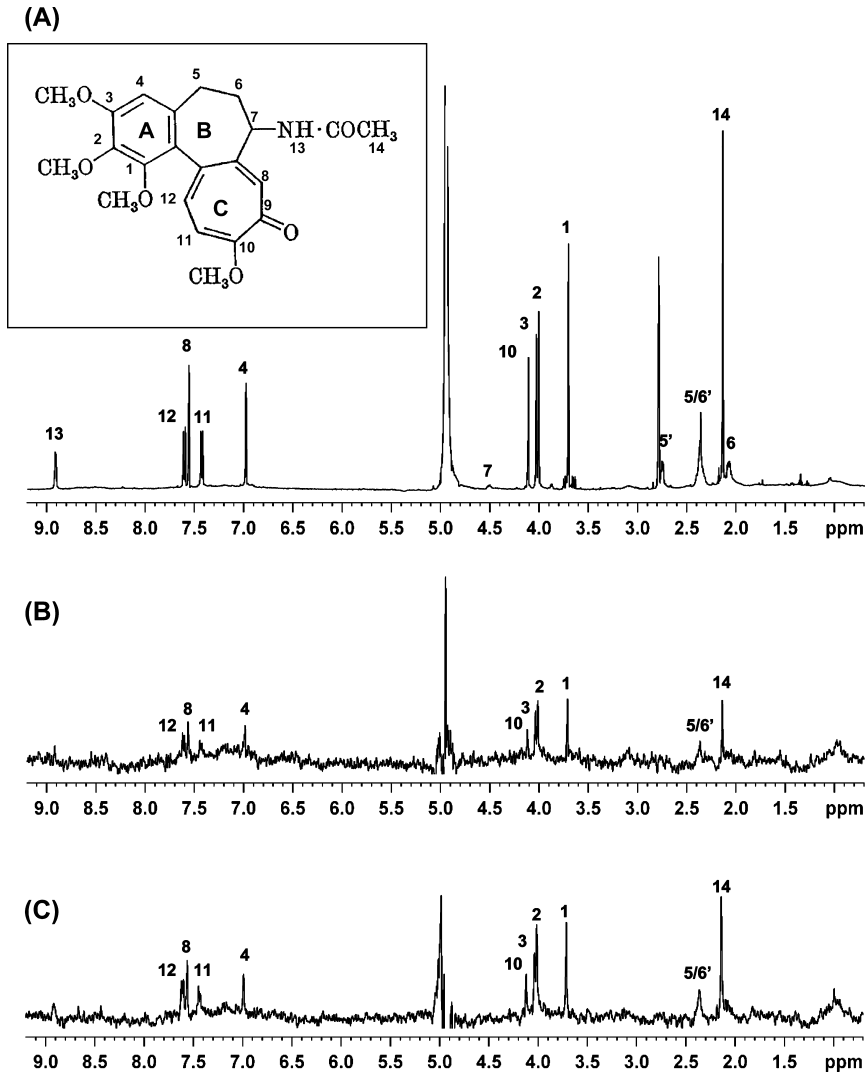

FIGURE 8: Binding of colchicine is enhanced in the presence of benomyl. (A) 1D ^{1}H NMR spectrum of colchicine in the presence of tubulin. The protons are labeled 1−14. The inset shows the structure of colchicine. (B and C) 1D STD−NMR spectra of colchicine in the presence of tubulin and tubulin preincubated with benomyl, respectively. The selective saturation of protein protons has been applied at 10 ppm. Protons of colchicine affected by the selective saturation of the protein are labeled.

Table 2: Comparison of STD Enhancements of Colchicine Protons in the Presence of Tubulin Preincubated with Benomyl or Not

ring	proton resonance	δ (ppm)	STD enhancement (%)[a] colchicine with tubulin	STD enhancement (%)[a] colchicine with tubulin−benomyl	benomyl/non-benomyl ratio
A	1-OMe	3.71	33	85	2.6
	2-OMe	4.01	43	96	2.2
	3-OMe	4.03	44	100	2.3
	4	6.98	32	83	2.6
B	5	2.79	0	0	0
	5′/6′	2.37	32	84	2.6
	6	2.08	23	53	2.3
	7	4.50	0	0	0
	13	8.92	26	53	2.0
	14	2.14	23	74	3.2
C	8	7.56	31	83	2.7
	10-OMe	4.11	29	74	2.6
	11	7.43	31	79	2.5
	12	7.61	39	100	2.6

[a] Normalized to the strongest enhancement, i.e., resonance 3-OMe in the presence of tubulin preincubated with benomyl.

Table 3: Comparison of the Interaction between Colchicine and Tubulin As Derived from the STD−NMR Experiments and Observed in the Tubulin−Colchicine−Stathmin-like Domain Crystal[a]

rank	NMR data: colchicine with tubulin	NMR data: colchicine with tubulin−benomyl	crystal structure[b]: protons	crystal structure[b]: no. of contacts
1	3-OMe (A)[c]	3-OMe (A)[c]/12 (C)	10-OMe (C)	136
2	2-OMe (A)[c]	2-OMe (A)[c]	2-OMe (A)[c]	116
3	12 (C)	1-O-Me (A)[c]	3-OMe (A)[c]	100
4	1-O-Me (A)[c]	5′ and/or 6′ (B)	1-O-Me (A)[c]	93
5	4 (A);[c] 5′ and/or 6′ (B)	4 (A);[c] 8 (C)	14 (B); 5 or 5′ (B)	40
6	8; 11 (C)	11 (C)	4 (A)[c]	38
7	10-OMe (C)	10-OMe (C); 14 (B)	11 (C)	37
8	13 (B)	13 (B); 6 (B)	6 or 6′ (B)	29
9	14 (B)	5; 7 (B)	5 or 5′ (B)	26
10	6 (B)		12 (C); 5 (B)	24
11	5; 7 (B)		8 (C)	20
12			6 or 6′ (B)	16
13			13 (B)	12

[a] Ranking of colchicine protons according to STD−NMR enhancement values and according to the number of intermolecular contacts (<5 Å) in the crystal structure. A, B, and C indicate the rings of colchicine. [b] From ref *25*. [c] Protons of colchicine ring A.

in the core of β-tubulin (*13, 33*). The conformational changes induced by benomyl and colchicine may facilitate and reinforce the interaction of each drug on β-tubulin. Therefore, the synergistic effects observed with benomyl and colchicine in cells may be explained by the cooperative interaction of both drugs on tubulin.

SUPPORTING INFORMATION AVAILABLE

1D spectra showing the degradation of benomyl in DMSO (Figures 1S and 2S) and the interaction of colchicine and tubulin in the presence of benomyl (Figure 3S). This material is available free of charge via the Internet at http://pubs.acs.org.

REFERENCES

1. Davidse, L. C. (1986) Benzimidazole fungicides: Mechanism of action and biological impact. *Annu. Rev. Phytopathol. 24*, 43–65.
2. Garcia-Sánchez, F., and Aguilar-Gallardo, A. (1994) Fluorimetric determination of the fungicide benomyl after solvolysis. *Mikrochim. Acta 116*, 211–218.
3. Chiba, M., and Veres, D. F. (1981) Fate of benomyl and its degradation compound methyl 2-benzimidazolecarbamate on apple foliage. *J. Agric. Food Chem. 29*, 588–590.
4. Davidse, L. C., and Flach, W. (1977) Differential binding of methyl benzimidazol-2-yl carbamate to fungal tubulin as a mechanism of resistance to this antimitotic agent in mutant strains of *Aspergillus nidulans*. *J. Cell Biol. 72*, 174–193.
5. Gupta, K., Bishop, J., Peck, A., Brown, J., Wilson, L., and Panda, D. (2004) Antimitotic antifungal compound benomyl inhibits brain microtubule polymerization and dynamics and cancer cell proliferation at mitosis, by binding to a novel site in tubulin. *Biochemistry 43*, 6645–6655.
6. Rathinasamy, K., and Panda, D. (2006) Suppression of microtubule dynamics by benomyl decreases tension across kinetochore pairs and induces apoptosis in cancer cells. *FEBS J. 273*, 4114–4128.
7. Kilmartin, J. V. (1981) Purification of yeast tubulin by self-assembly in vitro. *Biochemistry 20*, 3629–3633.
8. Singh, P., Rathinasamy, K., Mohan, R., and Panda, D. (2008) Microtubule assembly dynamics: An attractive target for anticancer drugs. *IUBMB Life 60*, 368–375.
9. Jordan, M. A., and Kamath, K. (2007) How do microtubule-targeted drugs work? An overview. *Curr. Cancer Drug Targets 7*, 730–742.
10. Rathinasamy, K., and Panda, D. (2008) Kinetic stabilization of microtubule dynamic instability by benomyl increases the nuclear transport of p53. *Biochem. Pharmacol.* , doi: 10.1016/j.bcp.2008.09.001.
11. Friedman, P. A., and Platzer, E. G. (1978) Interaction of anthelmintic benzimidazoles and benzimidazole derivatives with bovine brain tubulin. *Biochim. Biophys. Acta 544*, 605–614.
12. Friedman, P. A., and Platzer, E. G. (1980) Interaction of anthelmintic benzimidazoles with *Ascaris suum* embryonic tubulin. *Biochim. Biophys. Acta 630*, 271–278.
13. Downing, K. H. (2000) Structural basis for the interaction of tubulin with proteins and drugs that affect microtubule dynamics. *Annu. Rev. Cell Dev. Biol. 16*, 89–111.
14. Mayer, M., and Meyer, B. (1999) Characterization of Ligand Binding by Saturation Transfer Difference NMR Spectra. *Angew. Chem., Int. Ed. 35*, 1784–1788.
15. Panda, D., Rathinasamy, K., Santra, M. K., and Wilson, L. (2005) Kinetic suppression of microtubule dynamic instability by griseofulvin: Implications for its possible use in the treatment of cancer. *Proc. Natl. Acad. Sci. U.S.A. 102*, 9878–9883.
16. Chou, T. C., and Talalay, P. (1983) Analysis of combined drug effects: A new look at a very old problem. *Trends Pharmacol. Sci. 4*, 450–454.
17. Tyagi, A. K., Singh, R. P., Agarwal, C., Chan, D. C., and Agarwal, R. (2002) Silibinin strongly synergizes human prostate carcinoma DU145 cells to doxorubicin-induced growth Inhibition, G2-M arrest, and apoptosis. *Clin. Cancer Res. 8*, 3512–3519.
18. Chou, T. C., and Talalay, P. (1984) Quantitative analysis of dose-effect relationships: The combined effects of multiple drugs or enzyme inhibitors. *Adv. Enzyme Regul. 22*, 27–55.
19. Castoldi, M., and Popov, A. V. (2003) Purification of brain tubulin through two cycles of polymerization-depolymerization in a high-molarity buffer. *Protein Expression Purif. 32*, 83–88.
20. Detrich, H. W., and Williams, R. C. (1978) Reversible dissociation of the $\alpha\beta$ dimer of tubulin from bovine brain. *Biochemistry 17*, 3900–3917.
21. Piotto, M., Saudek, V., and Sklenar, V. (1992) Gradient-tailored excitation for single-quantum NMR spectroscopy of aqueous solutions. *J. Biomol. NMR 2*, 661–665.
22. Calmon, J. P., and Sayag, D. R. (1976) Kinetics and mechanisms of conversion of methyl 1-(butylcarbamoyl)-2-benzimidazolecarbamate (benomyl) to methyl 2-benzimidazolecarbamate (MBC). *J. Agric. Food Chem. 24*, 311–314.
23. Sassman, S. A., Lee, L. S., Bischoff, M., and Turco, R. F. (2004) Assessing N,N′-dibutylurea (DBU) formation in soils after application of n-butylisocyanate and benlate fungicides. *J. Agric. Food Chem. 52*, 747–754.
24. Lim, J., and Miller, M. G. (1997) The role of the benomyl metabolite carbendazim in benomyl-induced testicular toxicity. *Toxicol. Appl. Pharmacol. 142*, 401–410.
25. Morinaga, H., Yanase, T., Nomura, M., Okabe, T., Goto, K., Harada, N., and Nawata, H. (2004) A benzimidazole fungicide, benomyl, and its metabolite, carbendazim, induce aromatase activity in a human ovarian granulose-like tumor cell line (KGN). *Endocrinology 145*, 1860–1869.
26. Bane, S., Puett, D., Macdonald, T. L., and Williams, R. C., Jr. (1984) Binding to tubulin of the colchicine analog 2-methoxy-5-(2′,3′,4′-trimethoxyphenyl)tropone. Thermodynamic and kinetic aspects. *J. Biol. Chem. 259*, 7391–7398.
27. Andreu, J. M., Perez-Ramirez, B., Gorbunoff, M. J., Ayala, D., and Timasheff, S. N. (1998) Role of the colchicine ring A and its methoxy groups in the binding to tubulin and microtubule inhibition. *Biochemistry 37*, 8356–8368.
28. Bhattacharyya, B., Panda, D., Gupta, S., and Banerjee, M. (2008) Anti-mitotic activity of colchicine and the structural basis for its interaction with tubulin. *Med. Res. Rev. 28*, 155–183.
29. Ravelli, R. B. G., Gigant, B., Curmi, P. A., Jourdain, I., Lachkar, S., Sobel, A., and Knossow, M. (2004) Insight into tubulin regulation from a complex with colchicine and a stathmin-like domain. *Nature 428*, 198–202.
30. Detrich, H. W., III, Williams, R. C., Jr., Macdonald, T. L., Wilson, L., and Puett, D. (1981) Changes in the circular dichroic spectrum of colchicine associated with its binding to tubulin. *Biochemistry 20*, 5999–6005.
31. Hastie, S. B., Williams, R. C., Jr., Puett, D., and Macdonald, T. L. (1989) The binding of isocolchicine to tubulin. Mechanisms of ligand association with tubulin. *J. Biol. Chem. 264*, 6682–6688.
32. Hastie, S. B. (1989) Spectroscopic and kinetic features of allocolchicine binding to tubulin. *Biochemistry 28*, 7753–7760.
33. Fujimura, M., Oeda, K., Inoue, H., and Kato, T. (1992) A single amino-acid substitution in the β-tubulin gene of *Neurospora* confers both carbendazim resistance and diethofencarb sensitivity. *Curr. Genet. 21*, 399–404.

BI801136Q